DALTON
FULL PAPER

Utilization of crown ethers to stabilize the dinuclear μ-oxo bridged iron(III) aqua ion, $[(H_2O)_5Fe(\mu\text{-}O)Fe(OH_2)_5]^{4+}$ †

Peter C. Junk,*[a] Brian J. McCool,[b] Boujemaa Moubaraki,[a] Keith S. Murray,[a] Leone Spiccia,[a] John D. Cashion[c] and Jonathan W. Steed[d]

[a] *School of Chemistry, Box 23, Monash University, Victoria, 3800, Australia. E-mail: peter.junk@sci.monash.edu.au*
[b] *Department of Chemistry, James Cook University, Townsville, Queensland, 4811, Australia*
[c] *School of Physics and Materials Sciences, Box 27 Monash University, Victoria, 3800, Australia*
[d] *Department of Chemistry, King's College London, Strand, London, UK WC2R 2LS*

Received 28th June 2001, Accepted 3rd January 2002
First published as an Advance Article on the web 21st February 2002

Using a supramolecular approach a class of compounds containing the $[(H_2O)_5Fe–O–Fe(H_2O)_5]^{4+}$ core, *viz.* $[(H_2O)_5Fe–O–Fe(OH_2)_5](NO_3)_4\cdot(18\text{-crown-6})_2$, (**1**), $[(H_2O)_5Fe–O–Fe(OH_2)_5](ClO_4)_4\cdot(18\text{-crown-6})_2\cdot 2H_2O$ (**2**) and $[(H_2O)_5Fe–O–Fe(OH_2)_5](NO_3)_{10}[Fe(OH_2)_6]_2(15\text{-crown-5})_4\cdot(H_2O)_6$, (**3**), has been prepared and characterized. These three complexes were characterized by electronic, infrared, Raman and Mössbauer spectroscopy, X-ray crystallography and magnetic susceptibility. The X-ray structures reveal the crown ethers, anions and the $[(H_2O)_5Fe–O–Fe(H_2O)_5]^{4+}$ cores are all involved in extensive hydrogen bonding, thus stabilizing the unprecedented (in the solid state) dimeric cores. Magnetic susceptibility measurements show a strong antiferromagnetic coupling in each complex that is consistent with current radial and angular overlap descriptions of exchange coupling in mono-oxo bridged dinuclear Fe(III) complexes.

Introduction

The hydrolysis and polymerization of metal ions in aqueous media have been the focus of intense research activity for many decades.[1–4] This interest continues to be driven by the important role that hydrolytic processes play in the precipitation and dissolution of metal ions in aqueous environments. These include many aquatic systems,[1–4] biological systems,[5] where the storage and release of iron from the ferritin protein is one excellent example,[6,7] and numerous industrial processes,[4] (*e.g.*, the precipitation of alumina hydrate from Bayer liquors is critically dependent on solution speciation[8,9]). The understanding of the processes involved in the polymerization of metal ions at a molecular level is not commensurate with the recognized relevance of such processes. The considerable attention that has been directed at the metal ions with greatest technological impact, has led to a reasonable understanding of the solid phases that result from extensive polymerization and how these are converted into phases of varying crystallinity.[4,10,11] However, since this attention has, by necessity, focussed on the more labile metal ions, studies of the processes that take place in the early stages of hydrolysis, *i.e.* immediately following the addition of base to solutions of the aqua ions, are limited.

Taking advantage of the kinetic inertness of some trivalent metal ions (*e.g.*, $[Cr(OH_2)_6]^{3+}$, $[Rh(OH_2)_6]^{3+}$ and $[Ir(OH_2)_6]^{3+}$) a number of research groups have carried out detailed studies of the conversion of these aqua ions into polynuclear species.[12–19] These have included the use of various solution and solid state methods to establish the structures and thermodynamic and kinetic properties aimed at the establishment of reaction mechanisms for the formation, cleavage and interconversion reactions of each oligomer.

One of the major challenges in this area has been the design of effective synthetic methods for the crystallization of such polynuclear aqua ions. The high charge and ability to be strongly solvated in aqueous solution have been significant factors preventing the precipitation of the polynuclear ions. The most successful approach to be applied to date has involved the use of aromatic sulfonates in the crystallization of such aqua ions. It has been used in the crystallization of the Cr(III),[15] Sc(III)[20] and Rh(III)[17] dinuclear aqua ions, a heterometallic Cr(III)Rh(III) aqua ion,[21] an oxo bridged Mo(IV) trinuclear aqua ion[22] and numerous sulfido bridged polynuclear aqua ions.[23] Such aromatic anions enable the assembly of a superlattice, consisting of layers of the aqua ions separated by layers of the anions, which is stabilized through the formation of an extensive H-bonding network involving the aqua ions, unligated water molecules and the anions, and by interactions between the anions themselves.

The introduction of crown ethers, as agents which can further modify the H-bonding network that surrounds the metal aqua ions in aqueous solutions, has enabled the isolation of a novel crown ether adduct of the Cr(III) dimer mesitylate.[24] More recently, the combination of a sulfonated calixarene and a crown ether has facilitated the crystallization and structural elucidation of the Cr(III) trimer and tetramer for the first time.[25] Thus, in the case of Cr(III) it has been possible for the evolution of small oligomers to be followed at a molecular level.

Although the hydrolysis and polymerization of iron(III) in aqueous solution have been the subject of intense investigation since before the turn of this century,[1–4,6] and various products proposed to form in the early stages of polymerization, the constitution and structure of even the simplest oligomers are still subjects of debate. For example, the dinuclear iron(III) aqua ion has been proposed to have either a dihydroxy bridged core, $[(H_2O)_4Fe(\mu\text{-}OH)_2Fe(OH_2)_4]^{4+}$, or a single μ-oxo bridged core, $[(H_2O)_5Fe(\mu\text{-}O)Fe(OH_2)_5]^{4+}$.[4,6,26–28] Whilst the latter has been favored on the balance of magnetochemical and spectroscopic evidence, the interpretation of kinetic and thermodynamic

† Electronic supplementary information (ESI) available: diffuse reflectance UV-visible spectrum of complex **1**; hydrogen bonding data for compounds **1**, **2** and **3**. See http://www.rsc.org/suppdata/dt/b1/b105691n/

 DOI: 10.1039/b105691n

data, some of which have been reported very recently,[29] has often invoked the presence of the Fe(μ-OH)$_2$Fe core.

We report the X-ray structures, characterization and magnetic properties of three crown ether adducts of the dinuclear (μ-oxo)Fe^{III} cation, $[(H_2O)_5Fe(\mu\text{-}O)Fe(OH_2)_5]^{4+}$, isolated from aqueous solutions of $[Fe(OH_2)_6]^{3+}$, *viz.*, $[(H_2O)_5Fe–O–Fe(OH_2)_5](NO_3)_4\cdot$(18-crown-6)$_2$, **1**, $[(H_2O)_5Fe–O–Fe(OH_2)_5](ClO_4)_4\cdot$(18-crown-6)$_2\cdot 2H_2O$, **2** and $[(H_2O)_5Fe–O–Fe(OH_2)_5](NO_3)_{10}[Fe(OH_2)_6]_2$(15-crown-5)$_4\cdot(H_2O)_6$ (**3**). Apart from being the first examples of oxo-bridged dinuclear aqua ions to be structurally characterized, the existence of this ion provides strong evidence for its presence in hydrolyzing aqueous solutions of simple iron(III) salts. A preliminary account of the structure and magnetic properties of **1** has been communicated.[30]

Results and discussion

Synthesis

Slow evaporation of an aqueous solution of iron(III) nitrate in the presence of 18-crown-6 or 15-crown-5 deposited large orange crystals of a product whose elemental composition and IR spectrum indicated the presence of 18-crown-6 or 15-crown-5 molecules within the crystal lattice. Furthermore, a similar reaction product was obtained when 18-crown-6 was used in conjunction with iron(III) perchlorate rather than iron(III) nitrate. The X-ray crystal structures of these crystalline products confirmed the compositions $[(H_2O)_5Fe–O–Fe(OH_2)_5](NO_3)_4\cdot$(18-crown-6)$_2$, **1**, $[(H_2O)_5Fe–O–Fe(OH_2)_5](ClO_4)_4\cdot$(18-crown-6)$_2\cdot 2H_2O$, **2** and $[(H_2O)_5Fe–O–Fe(OH_2)_5](NO_3)_{10}[Fe(OH_2)_6]_2$(15-crown-5)$_4\cdot(H_2O)_6$ (**3**). The most exciting feature of these structures was the presence of the hitherto elusive dinuclear $[(H_2O)_5Fe–O–Fe(OH_2)_5]^{4+}$ aqua ion within the crystal lattice (Fig. 1).

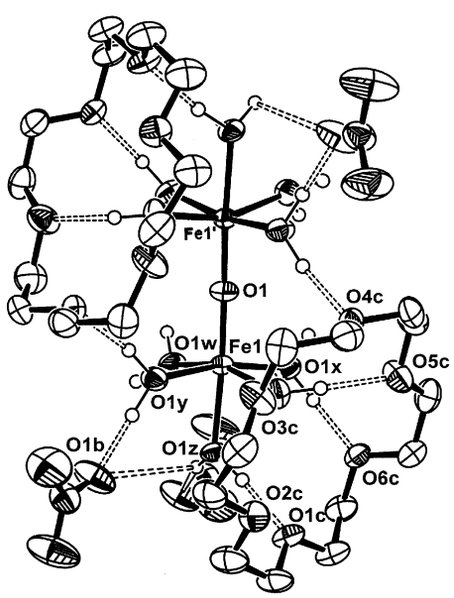

Fig. 1 Molecular structure of $[(H_2O)_5Fe–O–Fe(OH_2)_5](NO_3)_4\cdot$(18-crown-6)$_2$, **1** (ellipsoids are drawn at 50%).

The IR spectra of **1**, **2** and **3** show bands in the 3400 and 1600 cm^{-1} regions attributable respectively to OH stretches and bending of either water ligands or water of crystallization, and the bands expected for the nitrate and perchlorate counter-anions. The presence of the crown ethers is indicated by C–H stretches in the 2900 cm^{-1} region and low intensity C–C and C–O stretches in the 1000–1500 cm^{-1} region. The location of the asymmetric Fe–O–Fe vibration can be ascertained by comparing the IR and Raman spectra of the complexes, since it is IR active but Raman inactive. This vibration is clearly evident in the IR spectra, being located at 840 cm^{-1} for **1**, 841 cm^{-1} for **2** and 829 cm^{-1} for **3**. As has been found to be the case for other oxo-bridged Fe(III) derivatives, this vibration is not apparent in the Raman spectra. The location of these bands is as expected for complexes with linear or almost linear Fe–O–Fe units.[6,31] The symmetric Fe–O–Fe vibration, typically found in the 400–550 cm^{-1} region, could not be unambiguously assigned in either the IR or Raman spectra of the three complexes.

The diffuse reflectance UV-visible spectrum of **1** has been discussed earlier[30] and the spectra of **2** and **3** are similar (spectrum of **1** given in ESI †). A strong broad band centered at 380 nm, consisting of five component peaks between 210 and 430 nm, is similar to that reported by Solomon *et al.*[32] in a detailed analysis of [(HEDTA)FeOFe(HEDTA)]$^{2-}$, a μ-oxo complex first studied by Gray and Barraclough *et al.*[33] The band is assigned to oxo (p) ⟶ Fe^{III} (d) charge transfer transitions, with multiple peaks arising from excited state splittings. Variable temperature studies on single crystals of the present compounds would be required to deduce excited state energy separations caused by the antiferromagnetic coupling. A weaker broad band occurring at 799 nm is due to the spin forbidden d–d band $^6A_1 \longrightarrow {}^4T_1$ and it gains intensity from the low energy LMCT bands and from the covalent FeOFe moiety.[32] A shoulder on the low energy side of this band in the case of **3** might arise from the $[Fe(H_2O)_6]^{3+}$ cation. There are numerous bands of varying widths in the near IR region, 1000 to 2500 nm, but it is difficult to distinguish them from vibrational overtone bands.

X-Ray crystallography

X-Ray crystal structures of complexes **1**, **2** and **3** were studied and structure parameters are given in the Experimental section.

The molecular structure of **1** shows that the oxo bridging ligand lies on a two-fold rotation axis (Fig. 1). The iron centers are octahedral with five water molecules and the bridging oxo ligands completing each coordination sphere. The structure of this complex was discussed at length in a preliminary communication[30] and so will not be discussed in detail here. Selected bond lengths and angles are compiled in Table 1.

The overall structure involves a $[(H_2O)_5Fe–O–Fe(H_2O)_5]^{4+}$ cation which is stabilized by second-sphere hydrogen bonding interactions with the 18-crown-6 molecules (Fig. 1). In addition, there are several other hydrogen bonding contacts between the ligated waters (no waters of crystallization are present) and nitrate counter-anions. The crown ethers are hydrogen bonded to the remaining water molecules on $[(H_2O)_5Fe–O–Fe(H_2O)_5]^{4+}$ and each crown is bound to two water molecules on one Fe(III) and one water molecule on the other in an "ear-muff" fashion. Thus, by hydrogen bonding to water molecules ligated to both Fe(III) centers the 18-crown-6 macrocycle is imparting the stabilizing influence on the Fe–O–Fe unit that is required for isolation (in the solid state) of the unprecedented $[(H_2O)_5Fe–O–Fe(H_2O)_5]^{4+}$ ion.

The Fe–O–Fe angle of 170.2(4)° is intermediate for similar complexes (range 140 to 180°), but are generally in the range 170 to 180°.[34] The Fe–Fe distance of 3.549(2) Å is typical for complexes with mono bridged Fe–O–Fe cores, which are usually in the range 3.4–3.6 Å,[6,34] the longer values correlating with Fe–O–Fe angles that are linear or close to linearity.[6,34]

The molecular structure of compound **2** is closely related to **1** but in **2** the central oxygen atom of the $[(H_2O)_5Fe–O–Fe(OH_2)_5]^{4+}$ core lies on an inversion center giving an Fe–O–Fe angle of 180°. This is not atypical for related complexes. In contrast to the "ear-muff" type of encapsulation of the $[(H_2O)_5Fe–O–Fe(OH_2)_5]^{4+}$ core in **1**, the core in **2** is capped at either end by the 18-crown-6 macrocycles which are hydrogen-bonded to the terminal water ligands (see Fig. 2 and Table 2). The μ-O$_{(oxo)}$–Fe and O$_{(W)}$–Fe distances of 1.7752(3) Å and 2.0368(16) to 2.0884(15) Å respectively are in keeping with the mean values of 1.79 (with a range of 1.73 to 1.82 Å) and 2.09 Å

Table 1 Selected bond lengths (Å) and angles (°) for $[(H_2O)_5FeOFe(H_2O)_5](NO_3)_4\cdot(18\text{-crown-6})_2$, (**1**)

Fe(1)–O(1)	1.7809(11)	Fe(1)–O(1x)	2.040(4)
Fe(1)–O(1v)	2.055(4)	Fe(1)–O(1y)	2.051(4)
Fe(1)–O(1w)	2.057(4)	Fe(1)–O(1z)	2.114(4)
Fe(1) ··· Fe(1′)#1 [a]	3.549(2)		
O(1)–Fe(1)–O(1v)	101.26(18)	O(1v)–Fe(1)–O(1z)	80.74(17)
O(1)–Fe(1)–O(1w)	98.03(18)	O(1w)–Fe(1)–O(1x)	87.38(18)
O(1)–Fe(1)–O(1x)	96.41(17)	O(1w)–Fe(1)–O(1y)	93.85(18)
O(1)–Fe(1)–O(1y)	94.77(18)	O(1w)–Fe(1)–O(1z)	80.24(16)
O(1)–Fe(1)–O(1z)	176.54(13)	O(1x)–Fe(1)–O(1y)	168.48(16)
O(1v)–Fe(1)–O(1w)	160.15(17)	O(1z)–Fe(1)–O(1x)	86.54(16)
O(1v)–Fe(1)–O(1x)	85.85(17)	O(1y)–Fe(1)–O(1z)	82.39(16)
O(1v)–Fe(1)–O(1y)	89.22(17)	Fe(1)–O(1)–Fe(1′)#1 [a]	170.2(4)

[a] Symmetry transformations used to generate equivalent atoms: #1 $-x + 1, y, -z + 1.5$.

Table 2 Selected bond lengths (Å) and angles (°) for $[(H_2O)_5FeOFe(H_2O)_5](ClO_4)_4\cdot(18\text{-crown-6})_2\cdot 2H_2O$ (**2**)

Fe(1)–O(1)	2.0884(15)	Fe(1)–O(4)	2.0394(16)
Fe(1)–O(2)	1.7752(3)	Fe(1)–O(5)	2.0654(16)
Fe(1)–O(3)	2.0763(16)	Fe(1)–O(6)	2.0368(16)
Fe(1) ··· Fe(1′)#1 [a]	3.5504(3)		
O(1)–Fe(1)–O(2)	178.39(4)	O(2)–Fe(1)–O(6)	98.24(5)
O(1)–Fe(1)–O(3)	81.92(6)	O(3)–Fe(1)–O(4)	163.31(7)
O(1)–Fe(1)–O(4)	81.40(6)	O(3)–Fe(1)–O(5)	89.47(7)
O(1)–Fe(1)–O(5)	83.52(6)	O(3)–Fe(1)–O(6)	88.75(7)
O(1)–Fe(1)–O(6)	83.05(6)	O(4)–Fe(1)–O(5)	88.82(7)
O(2)–Fe(1)–O(3)	97.13(5)	O(4)–Fe(1)–O(6)	89.07(7)
O(2)–Fe(1)–O(4)	99.55(5)	O(5)–Fe(1)–O(6)	166.57(7)
O(2)–Fe(1)–O(5)	95.19(5)	Fe(1)–O(2)–Fe(1′)#1 [a]	180.0

[a] Symmetry transformations used to generate equivalent atoms: #1 $-x + 1, -y, -z + 1$.

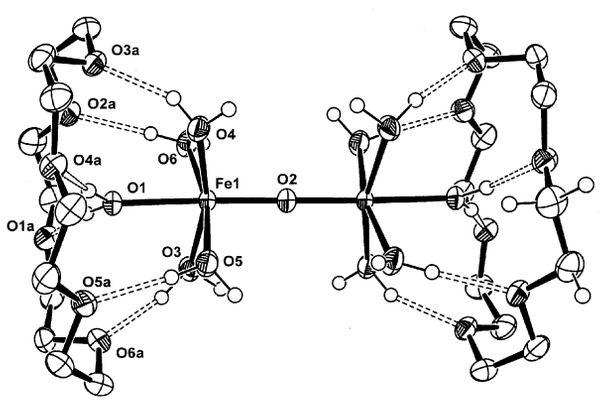

Fig. 2 ORTEP diagram showing second-sphere hydrogen bonding of the $[(H_2O)_5Fe–O–Fe(OH_2)_5]^{4+}$ fragment to the 18-crown-6 molecules in compound **2**. Perchlorate anions and lattice water molecules have been omitted for clarity (ellipsoids are drawn at 50%).

for such bond distances in iron(III)-oxo bridged complexes at room temperature.[34] The μ-$O_{(oxo)}$–Fe distance corresponds closely to that in **1** of 1.7809(11) Å. There is a *trans* influence exerted by the oxo ligand giving an axial $O_{(W)}$–Fe distance (2.088(1) Å) which is slightly longer than the $O_{(equat.)}$–Fe distances (ave = 2.054 Å) and the equatorial water molecules are bent away from the oxo ligand at an average of 97.5°. In line with the typical Fe ··· Fe distances (range = 3.4–3.6 Å)[6,34] in complexes with mono bridged Fe–O–Fe cores the Fe ··· Fe distance in complex **2** is 3.5504(3) Å.

As in compound **1**, the $[(H_2O)_5Fe–O–Fe(OH_2)_5]^{4+}$ cation is stabilized by second-sphere hydrogen bonding (supramolecular) interactions with the 18-crown-6 molecules (Fig. 2). In addition, there is an extensive hydrogen bonding network involving the ligated waters, the water molecules of crystallization, and perchlorate counter-anions (Fig. 2). The $[(H_2O)_5Fe–O–Fe(OH_2)_5]^{4+}$ core is hydrogen capped on either end by hydrogen bonding to 18-crown-6 molecules through the hydrogen atoms on water molecules O1, O3, O4, O5, and O6. The remaining hydrogen atoms on the $[(H_2O)_5Fe–O–Fe(OH_2)_5]^{4+}$ core are hydrogen bonded to the oxygen atoms of the perchlorate counterions (some of which span the water ligands on each Fe atom) and the water molecules of crystallization. Unlike compound **1** where a hydrogen bonded polymeric array forms between the waters of hydration and nitrate counterions, compound **2** exists as discrete dinuclear units with no significant inter-cation interactions (in compound **1** there are no *intermolecular* hydrogen bonding interactions involving the crown ethers, as was previously observed for the Cr(III) dimer adduct[24]). Thus, the capping of the dimers with 18-crown-6 molecules plays a critical role in stabilizing the $[(H_2O)_5Fe–O–Fe(OH_2)_5]^{4+}$ core in the solid state thereby facilitating crystallization. As in **1**, the oxo-bridge is not involved in hydrogen bonding interactions.

The molecular structure of compound **3** is related to those of **1** and **2** but there are some remarkable differences. The overall structure reveals the presence of one $[Fe(OH_2)_6]^{3+}$ ion sandwiched between two 15-crown-5 molecules. These 15-crown-5 molecules are also hydrogen bonded to water molecules located on the opposite side of the $[Fe(OH_2)_6]^{3+}$ cation which in turn are hydrogen bonded to nitrate counterions and the water molecules on the $[(H_2O)_5Fe–O–Fe(OH_2)_5]^{2+}$ cation (the nitrate anions are also involved in hydrogen bonding with the water molecules of hydration) (Fig. 3) (see Table 3 for selected bond lengths and angles). The overall structure is remarkable in that while the crown ether is required to stabilize/isolate the $[(H_2O)_5Fe–O–Fe(OH_2)_5]^{2+}$ core, it is not involved in direct hydrogen bonding to the water molecules of hydration (unlike compounds **1** and **2**), but in a third-sphere fashion. The reason for the incorporation of the $[Fe(OH_2)_6]^{3+}$ cation in **3**, and not in the 18-crown-6 adducts, is not clear but the ring size of the crown ether may be a contributing factor. Since the dinuclear cation in **3** appears to be stabilized by hydrogen bonds to nitrates and water molecules of crystallization, and not directly by the crown ether, it is remarkable that the $[(H_2O)_5Fe–O–Fe(OH_2)_5]^{4+}$ complex has not been isolated previously.

Table 3 Selected bond lengths (Å) and angles (°) for $[(H_2O)_5FeOFe(H_2O)_5](NO_3)_{10}[Fe(H_2O)_6]_2(15\text{-crown-}5)_4\cdot(H_2O)_6$ (**3**)

Fe(1)–O(1)	1.7803(4)	Fe(2)–O(7)	2.0061(17)
Fe(1)–O(2)	2.1358(18)	Fe(2)–O(8)	1.9820(17)
Fe(1)–O(3)	2.041(2)	Fe(2)–O(9)	2.0089(18)
Fe(1)–O(4)	2.0270(19)	Fe(2)–O(10)	1.9808(17)
Fe(1)–O(5)	2.054(2)	Fe(2)–O(11)	2.0030(17)
Fe(1)–O(6)	2.010(2)	Fe(2)–O(12)	1.9640(17)
Fe(1) ··· Fe(1′)#1 [a]	3.5610(2)		
O(1)–Fe(1)–O(2)	177.04(5)	O(7)–Fe(2)–O(8)	172.71(7)
O(1)–Fe(1)–O(3)	96.26(6)	O(7)–Fe(2)–O(9)	87.48(7)
O(1)–Fe(1)–O(4)	99.27(6)	O(7)–Fe(2)–O(10)	87.99(7)
O(1)–Fe(1)–O(5)	93.85(6)	O(7)–Fe(2)–O(11)	87.84(7)
O(1)–Fe(1)–O(6)	94.98(6)	O(7)–Fe(2)–O(12)	94.99(7)
O(2)–Fe(1)–O(3)	85.20(8)	O(8)–Fe(2)–O(9)	85.27(7)
O(2)–Fe(1)–O(4)	83.42(8)	O(8)–Fe(2)–O(10)	91.63(7)
O(2)–Fe(1)–O(5)	84.79(8)	O(8)–Fe(2)–O(11)	92.73(7)
O(2)–Fe(1)–O(6)	82.38(8)	O(8)–Fe(2)–O(12)	92.28(7)
O(3)–Fe(1)–O(4)	84.66(9)	O(9)–Fe(2)–O(10)	92.64(7)
O(3)–Fe(1)–O(5)	169.68(8)	O(9)–Fe(2)–O(11)	88.99(7)
O(3)–Fe(1)–O(6)	91.70(10)	O(9)–Fe(2)–O(12)	176.38(7)
O(4)–Fe(1)–O(5)	91.68(9)	O(10)–Fe(2)–O(11)	175.46(7)
O(4)–Fe(1)–O(6)	165.59(8)	O(10)–Fe(2)–O(12)	90.10(7)
O(5)–Fe(1)–O(6)	89.47(10)	O(11)–Fe(2)–O(12)	88.46(7)
Fe(1)–O(1)–Fe(1′)#1	180.0		

[a] Symmetry transformations used to generate equivalent atoms: #1 $-x, -y + 2, -z$.

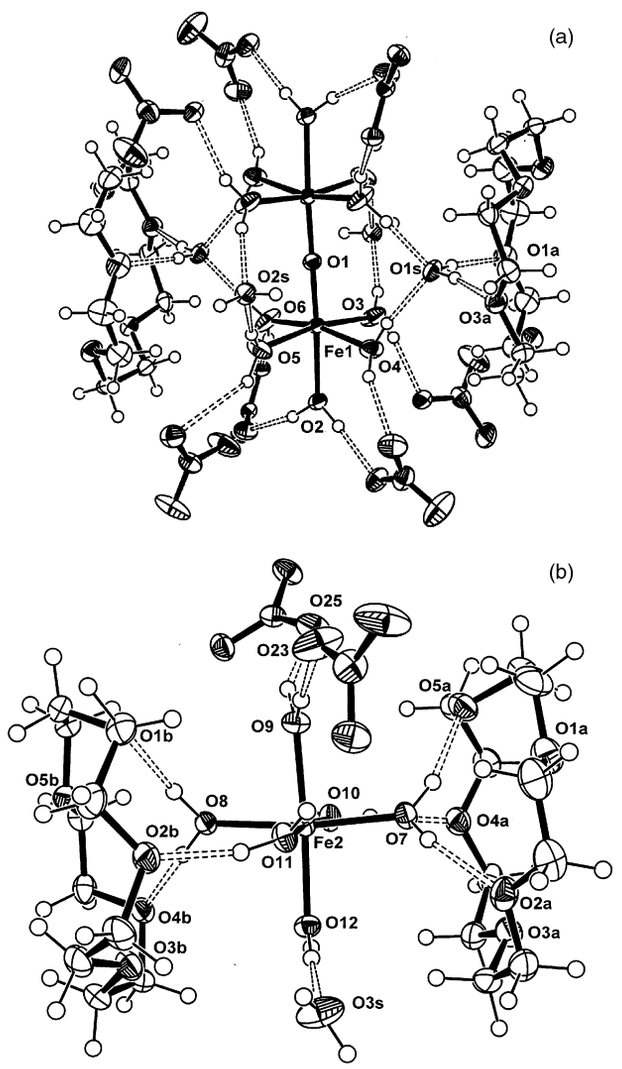

Fig. 3 (a) ORTEP diagram showing third-sphere hydrogen bonding of the $[(H_2O)_5Fe–O–Fe(OH_2)_5]^{4+}$ fragment to the 15-crown-5 molecules in compound **3** (ellipsoids are drawn at 50%). (b) ORTEP diagram showing second-sphere hydrogen bonding of the $[Fe(OH_2)_6]^{3+}$ fragment to the 15-crown-5 molecules in compound **3** (ellipsoids are drawn at 50%).

The $[(H_2O)_5FeOFe(OH_2)_5]^{4+}$ cation has similar geometric features to its analogue in compound **2** where the central oxygen atom lies on an inversion center giving an Fe–O–Fe angle of 180° (Fig. 3). The $\mu\text{-}O_{(oxo)}$–Fe distance of 1.7803(4) Å is similar to the corresponding distances in **1** and **2** of 1.7809(11) and 1.7752(3) Å; similarly the $O_{(W)}$–Fe distances of 2.010(2) to 2.136(2) Å in **3** are in good agreement with the corresponding distances in **1** and **2**. The *trans* influence exerted by the oxo ligand is again evident in compound **3** (and more significant than in compounds **1** and **2**) where the axial $O_{(W)}$–Fe distance (2.136(2) Å) is much longer than the $O_{(equat.)}$–Fe distances (ave = 2.033 Å) and the equatorial water molecules are bent away from the oxo ligand at an average of 96.1°. The Fe ··· Fe distance of 3.5610(2) Å is similar to those in compounds **1** and **2**.

Magnetism and Mössbauer spectrum

The 77 K Mössbauer spectrum of **1** showed a single, slightly asymmetric quadrupole doublet with isomer shift, δ, of 0.52 mm s^{-1}, quadrupole splitting, ΔE_Q, of 1.69 mm s^{-1}, line width at half height of 0.33 mm s^{-1} and area asymmetry (R/L) = 1.07 (Fig. 4). These are characteristic of high-spin d^5 systems, with the ΔE_Q value being at the high end of μ-oxo compounds having six-coordinate Fe(III).[6]

The strong antiferromagnetic coupling in complex **1** was discussed previously,[30] and the J value of -110 cm^{-1} compared favorably with that calculated using the angular and radial overlap model of Weihe and Güdel[35] which utilised the Fe–O–Fe angle and the average Fe–O distance. The plot of μ_{eff}, per Fe, *versus* temperature for **2** is shown in Fig. 5. The magnetic moments decrease, as expected, for strongly antiferromagnetically coupled $S = 5/2$ pairs. However, the plateau value of 1.7 μ_B between 60 to 20 K, is much higher than the value of zero expected, and reflected in a Curie-like tail in the corresponding susceptibilities. It arises due to a monomer impurity of 8.4%, much bigger than the 0.4% observed in **1**. Nevertheless, such behavior is not unknown in μ-oxo iron(III) systems[6,30,36] and a very good fit of the data was obtained. The best-fit parameters are $g = 2.02$, $J = -104$ cm^{-1}, % monomer 8.4, $\theta = -1.7$ K. The J value compares to that found, -107 cm^{-1}, for a μ-oxo complex of identical bridging geometry[37] and to the J_{model} value of -109 cm^{-1} calculated using the Weihe and Güdel model.[35] The θ value, included in the $(T - \theta)$ term of the susceptibility equation, reproduces the decrease in μ_{eff} values which is observed below 20 K. This parameter is often used as an indicator of weak dimer–dimer interactions and thus, if real, might

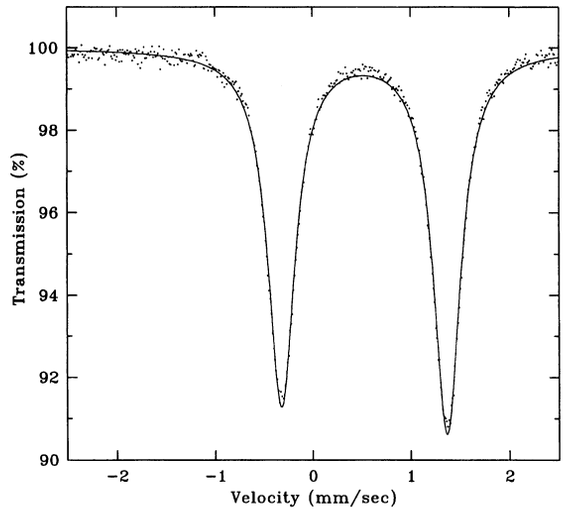

Fig. 4 Mössbauer effect spectrum of **1** measured at 77 K. The solid line is the fit to two singlets and the summation using the parameters given in the text.

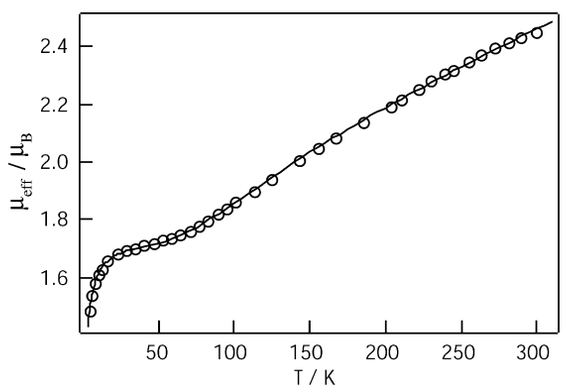

Fig. 5 Variation in magnetic moment, μ_{eff}, per Fe, with temperature for complex **2**. The observed data are shown as circles. The solid line is the calculated curve using the best-fit parameters discussed in the text.

indicate that such interactions are more significant than were noted in the structural details (*vide supra*).

Complex **3** contains a mole of $S = 5/2$ $[Fe(H_2O)_6]^{3+}$ per 2 moles (total) of Fe. Thus, the expected decrease in susceptibility with decreasing temperature for the $[(H_2O)_5Fe(\mu\text{-}O)Fe(H_2O)_5]^{4+}$ moiety, will be dominated by the Curie dependence of the susceptibility of the hexaaquairon(III) cation. This was observed, and the corresponding μ_{eff} values decreased only a little between 300 and 70 K before levelling off at a high value of μ_{eff} between 70 and 10 K. A rapid decrease in the magnetic moment was noted below 10 K, as in **2**. After subtracting off a susceptibility contribution of $4.375/T$ at each temperature (T) due to the $[Fe(H_2O)_6]^{3+}$ ion, the μ_{eff} *versus* T curve looked much like that in Fig. 5, except that the slope of the 300 to 70 K region was different. As in complex **2**, a non zero plateau remained between 70 and 10 K due to (further) monomer impurity. The plot could be reproduced reasonably well, although the g and J parameters were correlated and a θ value of *ca.* 28 K and a % monomer of *ca.* 5% were required. A $g = 1.96$ and $J = -152$ cm^{-1} combination, at best fit, has J too high, while a more reasonable J value of -120 cm^{-1} required an unreasonably low g value of 1.64. Too many parameters and corrections are involved in this dimer + $[Fe(H_2O)_6]^{3+}$ case to make any useful analysis.

Conclusion

This study demonstrates that the stabilization of the dinuclear $[(H_2O)_5Fe\text{–}O\text{–}Fe(OH_2)_5]^{4+}$ cation in the solid state by crown ether molecules may be a general phenomenon. These hitherto structurally uncharacterized species should allow a wealth of model studies to be performed on the simplest of these systems. The isolation of $[(H_2O)_5Fe\text{–}O\text{–}Fe(OH_2)_5]^{4+}$ in the solid state indicates that this cation is present in solution and provides scope for the re-examination of previous kinetic and thermodynamic studies.[29] Although the dihydroxo-bridged complex may possibly be the dominant species in solution, we have shown previously that the crown ether molecules can be used to crystallize species of this form of the dinuclear cation.[24]

The supramolecular approach detailed here should provide a convenient basis on which to synthesize more complex molecules containing the Fe–O–Fe sub-unit. In addition, it gives rise to the possibility of crystallizing elusive polynuclear aqua ions of other labile metal ions.

Experimental

Syntheses

$[(H_2O)_5Fe\text{–}O\text{–}Fe(OH_2)_5](NO_3)_4\cdot(18\text{-crown-}6)_2$, (1). Samples of $Fe(NO_3)_3\cdot 9H_2O$ (0.15 g, 0.38 mmol) and 18-crown-6 (0.10 g, 0.38 mmol) were dissolved in H_2O (5 cm^3) and allowed to evaporate at room temperature. Large orange crystals of **1** were isolated. (Found: C, 26.8; H, 6.9; N, 6.1. $C_{24}H_{68}O_{35}N_4Fe_2$ requires C, 26.6; H, 6.3; N, 5.2%). Infrared (KBr disk, ν/cm^{-1}): ~3400vs br, 2899m, 1638s, 1384vs, 1285m, 1248m, 1111vs, 1032w, 964s, 861w, 840s. Far infrared (vaseline mull, ν/cm^{-1}): 432m, 333w, 261m. Selected Raman bands (crystal ν/cm^{-1}): 2958s, 2919s, 1462w, 1274m, 1074w, 1035vs, 912w, 867m, 824w, 712w, 586w, 520w, 480w, 282m.

$[(H_2O)_5Fe\text{–}O\text{–}Fe(OH_2)_5](ClO_4)_4\cdot(18\text{-crown-}6)_2\cdot 2H_2O$ (2). Samples of $Fe(ClO_4)_3\cdot 6H_2O$ (0.18 g, 0.38 mmol) and 18-crown-6 (0.10 g, 0.38 mmol) were dissolved in H_2O (5 cm^3) and allowed to evaporate at room temperature. Orange crystals of **2** were isolated. (Found: C, 22.7; H, 6.1. $C_{24}H_{72}O_{41}Cl_4Fe_2$ requires C, 22.7; H, 5.7%). Infrared (KBr disk, ν/cm^{-1}): ~3400vs br, 2898m, 1637vs, 1476m, 1352m, 1284w, 1249w, 1115vs, 965m, 890w, 841m, 628m. Far infrared (vaseline mull, ν/cm^{-1}): 556w br, 540w, 476w br, 427m, 385w, 254s. Selected Raman bands (crystal ν/cm^{-1}): 2929vs, 1477m, 1284w, 1245w, 1131w, 1079w, 930vs, 860m, 821w, 626m, 459m, 373vs, 330vs.

$[(H_2O)_5Fe\text{–}O\text{–}Fe(OH_2)_5](NO_3)_{10}[Fe(OH_2)_6]_2(15\text{-crown-}5)_4\cdot(H_2O)_6$, (3). Samples of $Fe(NO_3)_3\cdot 9H_2O$ (0.15 g, 0.38 mmol) and 15-crown-5 (0.08 g, 0.38 mmol) were dissolved in H_2O (5 cm^3) and allowed to evaporate at room temperature. Large orange crystals of **3** were isolated. (Found: C, 21.7; H, 6.3; N, 5.8. $C_{20}H_{68}O_{39.5}N_5Fe_2$ requires C, 21.4; H, 6.1; N, 6.2%). Infrared (KBr disk, ν/cm^{-1}): 3450vs br, 2923w, 1638vs, 1543w, 1384vs, 1249m, 1118vs, 1096vs, 1039m, 947s, 861w, 829m. Far infrared (vaseline mull, ν/cm^{-1}): 552w, 512w, 453w br, 366m, 316m, 261vs, 203m. Selected Raman bands (crystal ν/cm^{-1}): 2945s, 2892s, 1474m, 1280m, 1248m, 1135w, 1047vs, 857s, 722w, 552w, 369w, 292m.

Crystallography

Single crystals of **1** were sealed in thin walled glass capillaries while **2** and **3** were mounted on thin glass fibers. For **1**, final lattice parameters as determined from the least-squares refinement of the angular settings of 25 high angle reflections ($2\theta > 30°$) accurately centered on an Enraf-Nonius CAD4 diffractometer are given below. No absorption correction was required. For compounds **2** and **3**, final lattice parameters and data collection information are given below. Data were collected on a Nonius ^{Kappa}CCD diffractometer, absorption corrections were performed using Scalepack and calculations for all compounds were carried out using the SHELX97 suite of computer programs[38] (refinement by full-matrix least squares techniques on F^2) with the aid of the program RES2INS.[39]

The positions of heavy atoms in all compounds were determined from a three-dimensional Patterson function. All other non-hydrogen atoms were located from a difference-Fourier synthesis and were refined anisotropically. For compound **1**, hydrogen atoms were placed at calculated positions and their parameters were not refined. For compounds **2** and **3**, all hydrogen atoms were located and refined isotropically. Refinements converged with $R = 0.056$ for 1839 observed reflections for **1**, $R = 0.0419$ for 4784 observed reflections for **2**, and $R = 0.0536$ for 8780 observed reflections for **3**.

Crystal data for 1. $C_{24}H_{68}O_{35}N_4Fe_2$, $M = 1084.51$, monoclinic, space group $C2/c$ (#15), $a = 22.863(3)$, $b = 10.993(1)$, $c = 20.758(4)$ Å, $\beta = 111.02(1)°$, $U = 4870(1)$ Å^3, $D_c = 1.479$ g cm^{-3}, $T = 296$ K, $Z = 4$, $F(000) = 2288$, $\mu_{Mo} = 0.69$ mm^{-1}, number of reflections collected = 4383, number of unique reflections = 4268 ($R_{int} = 0.062$), $R1$ [$I > 2\sigma(I)$] = 0.0646, $wR2$ (all data) = 0.1534.

CCDC reference number 174787.

Crystal data for 2. $C_{24}H_{72}Cl_4O_{41}Fe_2$, $M = 1270.32$, triclinic, space group $P\bar{1}$ (#2), $a = 10.2655(7)$, $b = 12.2247(6)$, $c = 12.2953(6)$ Å, $\alpha = 71.820(2)$, $\beta = 72.129(2)$, $\gamma = 66.353(2)°$, $U = 1313.3(1)$ Å^3, $D_c = 1.606$ g cm^{-3}, $T = 173(2)$ K, $Z = 1$, $F(000) = 664$, $\mu_{Mo} = 0.86$ mm^{-1}, number of reflections collected = 10996, number of unique reflections = 4784 ($R_{int} = 0.025$), $R1$ [$I > 2\sigma(I)$] = 0.0364, $wR2$ (all data) = 0.0965.

CCDC reference number 149181.

Crystal data for 3. $C_{20}H_{68}O_{39.5}N_5Fe_2$, $M = 1122.49$, monoclinic, space group $P2_1/a$ (#14), $a = 15.7399(7)$, $b = 14.7129(4)$, $c = 22.004(1)$ Å, $\beta = 110.86(1)°$, $U = 4761.5(3)$ Å^3, $D_c = 1.566$ g cm^{-3}, $T = 123(2)$ K, $Z = 4$, $F(000) = 2364$, $\mu_{Mo} = 0.72$ mm^{-1}, number of reflections collected = 16428, number of unique reflections = 8780 ($R_{int} = 0.034$), $R1$ [$I > 2\sigma(I)$] = 0.0434, $wR2$ (all data) = 0.1160.

CCDC reference number 149182.

See http://www.rsc.org/suppdata/dt/b1/b105691n/ for crystallographic data in CIF or other electronic format.

Physical measurements

Electronic spectra were measured in diffuse reflectance mode using a Cary 5G instrument (Varian) over the ranges 200 to 1000 nm and 400 to 2500 nm. Infrared spectra were recorded as KBr pellets on a Perkin Elmer 1600 FTIR spectrometer and far infrared spectra as vaseline mulls on a Bruker IFS120 FTIR spectrometer. The resolution employed was 4 cm^{-1}. Raman spectra were measured on a Renishaw Ramascope System 2000 fitted with a He–Ne laser.

Magnetic susceptibilities were measured on powdered samples contained in calibrated gelatine capsules using a Quantum Design MPMS 5 SQUID magnetometer operating in a field of 1 T. The instrument was calibrated against a standard Pd sample supplied by the company and against a chemical calibrant $CuSO_4 \cdot 5H_2O$.

Mössbauer spectra were measured and fitted by Associate Professor J. D. Cashion, Department of Physics, Monash University using equipment described previously.[40]

Acknowledgements

Financial support from the Australian Research Council is gratefully acknowledged. We thank Mr Finlay Shanks for the far infrared and Raman measurements.

References

1 C. F. Baes, Jr. and R. E. Mesmer, *The Hydrolysis of Cations*, Wiley Interscience, New York, 1976, and references cited therein.
2 W. Stumm and J. J. Morgan, *Aquatic Chemistry*, 3rd edn., Wiley Interscience, New York, 1996.
3 W. Schneider and B. Schwyn, in *Aquatic Surface Chemistry*, ed. W. Stumm, Wiley, New York, 1987, p. 167.
4 R. N. Sylva, *Rev. Pure Appl. Chem.*, 1972, **22**, 115.
5 S. J. Lippard and J. M. Berg, *Principles of Bioinorganic Chemistry*, University Science Books, Mill Valley, CA, 1994.
6 D. M. Kurtz, Jr., *Chem. Rev.*, 1990, **90**, 585.
7 K. S. Hagen, *Angew. Chem., Int. Ed. Engl.*, 1992, **31**, 1010; A. K. Powell, *Struct. Bonding (Berlin)*, 1997, **88**, 1.
8 S. Kumar and R. G. Bautista, in *Light Metals 1994*, ed. U. Mannweiler, The Minerals, Metals and Materials Society, Warrendale, PA, 1994, p. 47.
9 W. J. Crama and J. Visser, in *Light Metals 1994*, ed. U. Mannweiler, The Minerals, Metals and Materials Society, Warrendale, PA, 1994, p. 73.
10 W. Schneider, *Comments Inorg. Chem.*, 1984, **3**, 205.
11 R. W. Cornell, R. Giovanoli and W. Schneider, *J. Chem. Technol. Biotechnol.*, 1989, **46**, 115.
12 M. Ardon and G. Stein, *J. Chem. Soc.*, 1956, 2095; M. Ardon and R. A. Plane, *J. Am. Chem. Soc.*, 1959, **81**, 3197; M. Ardon and A. Linenberg, *J. Phys. Chem.*, 1961, **65**, 1443; R. W. Kolaczkowski, *Inorg. Chem.*, 1964, **3**, 322.
13 M. E. Thompson and R. E. Connick, *Inorg. Chem.*, 1981, **20**, 2279; J. E. Finholdt, R. E. Thompson and R. E. Connick, *Inorg. Chem.*, 1981, **20**, 4151.
14 H. Stünzi and W. Marty, *Inorg. Chem.*, 1983, **22**, 2145; H. Stünzi, F. P. Rotzinger and W. Marty, *Inorg. Chem.*, 1984, **23**, 2160; L. Spiccia and W. Marty, *Inorg. Chem.*, 1986, **25**, 489; L. Spiccia, W. Marty and R. Giovanoli, *Inorg. Chem.*, 1988, **27**, 2660.
15 L. Spiccia, H. Stoeckli-Evans, W. Marty and R. Giovanoli, *Inorg. Chem.*, 1987, **26**, 474.
16 T. Merakis and L. Spiccia, *Aust. J. Chem.*, 1989, **42**, 1579; H. Stünzi, L. Spiccia, F. P. Rotzinger and W. Marty, *Inorg. Chem.*, 1989, **28**, 66; L. Spiccia and W. Marty, *Polyhedron*, 1991, **10**, 619; L. Spiccia, *Polyhedron*, 1991, **10**, 1865; S. J. Crimp, L. Spiccia, H. R. Krouse and T. W. Swaddle, *Inorg. Chem.*, 1994, **33**, 465; A. Drljaca and L. Spiccia, *Polyhedron*, 1995, **14**, 1653; A. Drljaca and L. Spiccia, *Polyhedron*, 1996, **15**, 2875; A. Drljaca, L. Spiccia, H. R. Krouse and T. W. Swaddle, *Inorg. Chem.*, 1996, **35**, 985.
17 R. Cervini, G. D. Fallon and L. Spiccia, *Inorg. Chem.*, 1991, **30**, 831.
18 L. Spiccia, J. M. Aramini, S. J. Crimp, A. Drljaca, E. T. Lawrenz, V. Tedesco and H. J. Vogel, *J. Chem. Soc., Dalton Trans.*, 1997, 4603.
19 S. E. Castillo-Blum, D. T. Richens and A. G. Sykes, *Inorg. Chem.*, 1989, **28**, 954.
20 F. Matsumoto, Y. Ohki, Y. Suzuki and A. Ouchi, *Bull. Chem. Soc. Jpn.*, 1989, **62**, 2081.
21 S. J. Crimp, G. D. Fallon and L. Spiccia, *J. Chem. Soc., Chem. Commun.*, 1992, 197.
22 D. T. Richens, L. Helm, P.-A. Pittet, A. E. Merbach, F. Nicoló and G. Chapuis, *Inorg. Chem.*, 1989, **28**, 1394.
23 See for example: T. Shibahara, H. Akashi and H. Kuroya, *J. Am. Chem. Soc.*, 1998, **110**, 3313; H. Akashi and T. Shibahara, *Inorg. Chem.*, 1989, **28**, 2906; T. Shibahara and M. Yamasaki, *Inorg. Chem.*, 1991, **30**, 1687; T. Shibahara, M. Yamasaki, T. Watase and A. Ichimura, *Inorg. Chem.*, 1994, **33**, 292 and references therein.
24 A. Drljaca, D. C. R. Hockless, B. Moubaraki, K. S. Murray and L. Spiccia, *Inorg. Chem.*, 1997, **36**, 1988–1989.
25 A. Drljaca, M. J. Hardie, C. L. Raston and L. Spiccia, *Chem. Eur. J.*, 1999, **5**, 2295.
26 M. Magini, A. Saltetti and R. Caminiti, *Inorg. Chem.*, 1981, **20**, 3564.
27 F. A. Cotton and G. Wilkinson, *Advanced Inorganic Chemistry*, 5th edn., Wiley-Interscience, New York, 1987, p. 717.
28 N. N. Greenwood and A. Earnshaw, *Chemistry of the Elements*, Pergamon Press, Oxford, 1984, p. 1265.
29 G. Lente and I. Fabian, *Inorg. Chem.*, 1999, **38**, 603 and references therein.
30 P. C. Junk, B. J. McCool, B. Moubaraki, K. S. Murray and L. Spiccia, *Angew. Chem., Int. Ed.*, 1999, **38**, 2224.
31 G. Haselhorst, K. Wieghardt, S. Keller and B. Schrader, *Inorg. Chem.*, 1993, **32**, 520.
32 C. A. Brown, G. J. Remar, R. L. Musselman and E. I. Solomon, *Inorg. Chem.*, 1995, **34**, 688.
33 H. J. Schugar, G. R. Rossman, C. G. Barraclough and H. B. Gray, *J. Am. Chem. Soc*, 1972, **94**, 2683.
34 A. G. Orpen, L. Brammer, F. H. Allen, O. Kennard, D. G. Watson and R. Taylor, *J. Chem. Soc., Dalton Trans.*, 1989, S1.
35 H. Weihe and H. Güdel, *J. Am. Chem. Soc.*, 1997, **119**, 6539.
36 K. S. Murray, *Coord. Chem. Rev.*, 1974, **12**, 1.
37 C. C. Ou, R. G. Wollmann, D. N. Hendrickson, J. A. Potenza and H. J. Schugar, *J. Am. Chem. Soc.*, 1978, **100**, 4717.
38 G. M. Sheldrick, SHELXL-97, University of Göttingen, 1997.
39 L. J. Barbour, RES2INS, University of Missouri, Columbia, 1995.
40 S. Sievertsen, K. S. Murray, B. Moubaraki, K. J. Berry, Y. Korbatieh, J. D. Cashion, L. J. Brown and H. Homborg, *Z. Anorg. Allg. Chem.*, 1994, **620**, 1203.